SPHERE: a 'Planet Finder' instrument for the VLT

Jean-Luc Beuzit[*a], Markus Feldt[b], Kjetil Dohlen[c], David Mouillet[a], Pascal Puget[a], Francois Wildi[d], Lyu Abe[e], Jacopo Antichi[f], Andrea Baruffolo[f], Pierre Baudoz[g], Anthony Boccaletti[g], Marcel Carbillet[e], Julien Charton[a], Riccardo Claudi[f], Mark Downing[h], Christophe Fabron[c], Philippe Feautrier[a], Enrico Fedrigo[h], Thierry Fusco[i], Jean-Luc Gach[c], Raffaele Gratton[f], Thomas Henning[b], Norbert Hubin[h], Franco Joos[k], Markus Kasper[h], Maud Langlois[c], Rainer Lenzen[b], Claire Moutou[c], Alexey Pavlov[b], Cyril Petit[i], Johan Pragt[j], Patrick Rabou[a], Florence Rigal[j], Ronald Roelfsema[j], Gérard Rousset[g], Michel Saisse[c], Hans-Martin Schmid[k], Eric Stadler[a], Christian Thalmann[k], Massimo Turatto[f], Stéphane Udry[d], Farrokh Vakili[e], Rens Waters[l]

[a] LAOG, UMR5571, CNRS/Université J. Fourier, B.P. 53, F-38041 Grenoble Cedex 9, France;
[b] Max Planck Institüt für Astronomie, Königsthul 17, D-69117 Heidelberg, Germany;
[c] LAM, UMR6110, CNRS/Université de Provence, B.P. 8, F-13376 Marseille Cedex 12, France;
[d] Observatoire de Genève, 51 chemin des Maillettes, CH-1290 Sauverny, Switzerland;
[e] Laboratoire H. Fizeau, UNS/CNRS/OCA, Campus Valrose, F-06108 Nice Cedex 2, France;
[f] Osservatorio Astronomico di Padova, INAF, Vicolo dell'Osservatorio 5, I-35122 Padova, Italy;
[g] LESIA, CNRS/Observatoire de Paris, 5 place J. Janssen, F-92190 Meudon, France;
[h] European Southern Observatory, Karl-Schwarzschild-Strasse 2, D-85748 Garching, Germany;
[i] Office National d'Etudes et de Recherches Aérospatiales, B.P. 72, F-92322 Chatillon, France;
[j] NOVA/ASTRON, Oude Hoogeveensedijk 4, NL-7990 PD Dwingeloo, The Netherlands;
[k] Institute of Astronomy, ETH Zurich, CH-8092 Zurich, Switzerland;
[l] Universität van Amsterdam, Kruislaan 403, NL-1098 SJ Amsterdam, The Netherlands

ABSTRACT

Direct detection and spectral characterization of extra-solar planets is one of the most exciting but also one of the most challenging areas in modern astronomy. The challenge consists in the very large contrast between the host star and the planet, larger than 12.5 magnitudes at very small angular separations, typically inside the seeing halo. The whole design of a "Planet Finder" instrument is therefore optimized towards reaching the highest contrast in a limited field of view and at short distances from the central star. Both evolved and young planetary systems can be detected, respectively through their reflected light and through the intrinsic planet emission. We present the science objectives, conceptual design and expected performance of the SPHERE instrument.

Keywords: extrasolar planets, extreme adaptive optics, coronagraphy, dual imaging, polarimetry, spectral imaging

1. INTRODUCTION

The prime objective of the Spectro-Polarimetric High-contrast Exoplanet Research (SPHERE) instrument for the VLT is the discovery and study of new extra-solar giant planets orbiting nearby stars by direct imaging of their circumstellar environment. The challenge consists in the very large contrast between the host star and the planet, larger than 12.5 magnitudes (or 10^5 in flux ratio), at very small angular separations, typically inside the seeing halo. The whole design of SPHERE is therefore optimized towards reaching the highest contrast in a limited field of view and at short distances from the central star. Both evolved and young planetary systems will be detected, respectively through their reflected light (mostly by visible differential polarimetry) and through the intrinsic planet emission (using IR differential imaging and integral field spectroscopy). Both components of the near-infrared arm of SPHERE will provide complementary detection capabilities and characterization potential, in terms of field of view, contrast, and spectral domain.

---

[*] Jean-Luc.Beuzit@obs.ujf-grenoble.fr

1.1. Science objectives

The primary goal of extra-solar planet science of the next decade will be a better understanding of the mechanisms of formation and evolution of planetary systems. The fundamental observational parameter is the frequency of planets as a function of mass and separation. Theoretical models of planet formation predict that the peak of formation of giant planets is found close to the snowline, thanks to the availability of a larger amount of condensate in the proto-planetary disk. In outer regions, the longer timescales involved should make planet formation a less efficient process. Migration mechanisms and long term orbit instabilities will alter the original distribution. Determination of the frequency of giant planets in wide orbits (> 5-10 AU) will allow testing basic aspects of the planet formation models.

While radial velocity spectroscopy remains the best technique currently available to study the inner side of the planet distribution with semi-major axis (<5 AU), high-resolution, high contrast imaging like that provided by SPHERE is expected to be the most efficient technique to discover planets in the outer regions of planetary systems (Fig. 1). Current results from direct imaging surveys allow excluding only planet distributions with a large population of massive planets in outer orbits. With its enhanced capabilities (a gain of two orders of magnitudes in contrast with respect to existing instruments) and a list of potential targets including several hundred stars, SPHERE will provide a clear view of the frequency of giant planets in wide orbits. With the number of expected detections (several tens), the level of the large separation wing of the distribution with semi-major axis can probably be estimated with an accuracy of about 20-30%, good enough for a first statistical discussion of the properties of planetary systems. Beside frequency, it would also be interesting to derive the distributions of planets parameters such as mass, semi-major axis and eccentricities.

The main scientific goal of SPHERE will be then the description of the properties of young planets in the expected peak region of gas giant formation and in the outer regions of the systems. Imaging of planets already detected by radial velocity and/or astrometry would additionally represent a major breakthrough thanks to the availability of dynamical constraints (or even full orbit determinations) on the planet masses and on the orbital elements. Therefore, these objects will represent the ideal benchmarks for the calibration of models for sub-stellar objects.

Furthermore, a direct imager like SPHERE provides the only way of obtaining spectral characteristics for outer planets. Finally, the SPHERE differential polarimetric channel (ZIMPOL) might allow detecting a few planets shining by reflecting stellar light. Such an instrument will then provide invaluable information with which to hone models in preparation for the Darwin and ELT era. SPHERE will be then highly complementary to current and contemporaneous studies of extrasolar planets.

An instrument with the capabilities to achieve these goals will also be able to make great advances in related areas of study such as brown dwarfs, star and planet formation (e.g. via imaging of disks), Solar System objects (asteroids), etc. These domains will nicely enrich the scientific impact of the instrument. Their instrumental needs should however not be in conflict with the high-contrast requirements.

1.2. Target classes

These science objectives fully justify a large effort in an extended observational survey of several hundred nights concentrating on the following classes of targets:

- *Nearby young associations (10-100 Myr, 30-100pc)* will offer the best chance of detecting low mass planets, since they will have brighter sub-stellar companions.
- *Young active F-K dwarfs* of the Solar neighbourhood (ages less than 1 Gyr, d < 50pc).
- *Nearest stars* (all ages within 20pc of the Sun) will allow probe the smallest orbits and will also be the only opportunities for detecting planets by directly reflected light.
- *Stars with known planets*, especially any that exhibit long-term residuals in their radial velocity curves, indicating the possible presence of a more distant planet (F-G-K stars within 50-100pc).
- *Young early type stars.*
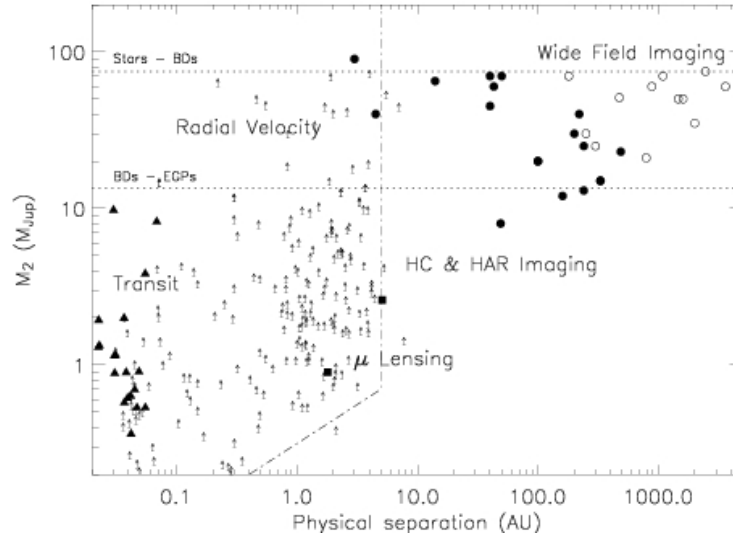- *Planet candidates from astrometric surveys*.

Fig. 1. SPHERE extra-solar planets discovery space compared to other techniques: radial velocity (arrows), transit (filled triangles), micro lensing (filled boxes), wide field imaging (open circles) and high contrast and high dynamic range imaging (filled circles)

1.3. High level requirements

The key high level requirements derived from the science analysis and driving the design of the instrument are summarized below:

- High contrast capability to detect giant planets 15 magnitudes fainter than their host star at 0.5'' (for host stars with J < 6).
- Access to very small angular separations, 0.1" to 3" from the host star.
- Optimal performance for targets up to visible magnitude ~ 9, for building a large enough target list (a few hundred targets).
- Access to an extended spectral domain at low resolution, for the characterization of the detected objects, at a resolving power ~ 30.
- Sensitivity to extended sources down to ~ 17 magnitudes per arcsecond^2 at less than 0.2" from the host star.

2. SYSTEM OVERVIEW AND COMMON PATH

The proposed design of SPHERE is divided into four subsystems: the Common Path and Infrastructure (CPI) and the three science channels, a differential imaging camera (IRDIS, InfraRed Dual Imaging Spectrograph), an Integral Field Spectrograph (IFS) and a visible imaging polarimeter (ZIMPOL, Zurich Imaging Polarimeter). The Common Path includes pupil stabilizing fore optics (tip-tilt and rotation), calibration units, the SAXO extreme adaptive optics system, and NIR and visible coronagraphic devices. ZIMPOL shares the visible channel with the wavefront sensor through a beamsplitter, which can be a grey (80% to ZIMPOL) beamsplitter, a dichroic beamsplitter, or a mirror (no ZIMPOL observations). IRDIS is the main science channel responsible for wide-field imaging in one or two simultaneous spectral bands or two orthogonal polarizations and low and medium resolution long slit spectroscopy. The IFS, working from 0.95 to 1.65 µm, provides low spectral resolution (R ~ 30) over a limited, 1.8" x 1.8", field-of-view. A photon sharing scheme has been agreed between IRDIS and IFS, allowing IFS to exploit the NIR range up to the J band, leaving the H-band, judged optimal for the DBI mode, for IRDIS for the main observation mode. This multiplexing optimizes the observational efficiency. This global concept is illustrated in Fig. 2 and the current implementation of SPHERE at the Nasmyth focus of the VLT is shown in Fig. 3.
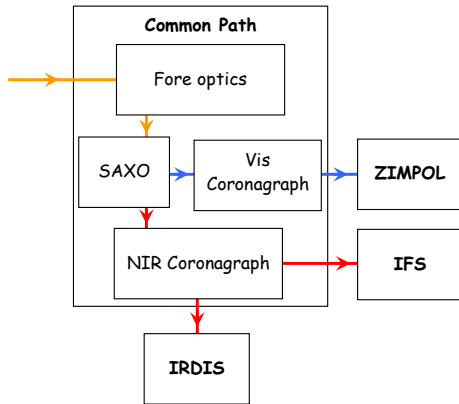
Fig. 2. The four sub-systems of SPHERE. Optical beams are indicated in red for NIR, blue for visible and orange for CPI.
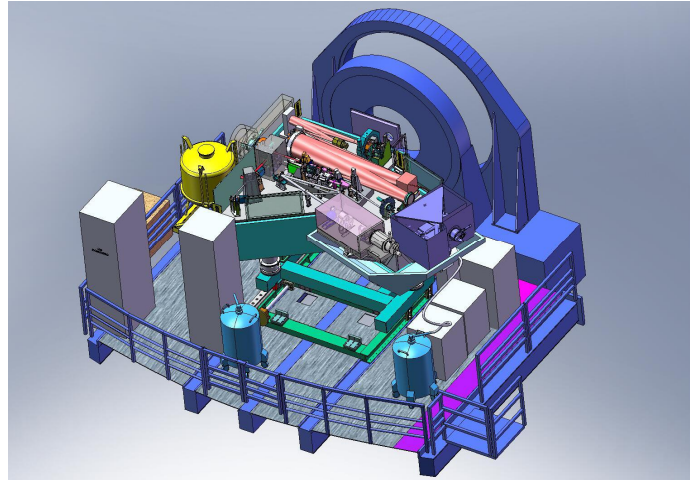

Fig. 3. SPHERE implementation on the Nasmyth platform of the VLT.

2.1. Common Path and Infrastructure (CPI)

The common path will be mounted on a large actively damped optical bench to which each science instrument will dock as a whole. When in operation on one of the VLT Nasmyth platforms, SPHERE will be entirely enclosed in a thermal/dust cover and include a comprehensive automated cryo-vacuum system supplying 4 cryostats and a separate vacuum container.

Besides classical optical components, the common path embeds numerous new high-technology components like a high order deformable mirror from CILAS, toroidal mirrors manufactured by spherical polishing of pre-stressed substrates[1], a dedicated electron multiplying CCD for wavefront sensing, achromatic 4 quadrants coronagraph, classical and apodized Lyot coronagraphs. A good number of these components have one or more of their degrees of freedom motorized, for a total of around 60 motors.

2.2. Extreme adaptive optics (SAXO)

Three loops and one off line calibration compose the SAXO[2] extreme adaptive optics system (Fig. 4).

- The main AO loop corrects for atmospheric, telescope and common path defects. The main impact is the increase of detection signal to noise ratio through the reduction of the smooth PSF halo due to turbulence effects.

- The Differential Tip-Tilt loop ensures a fine centering of the beam on the coronagraphic mask (correction of differential tip-tilt between VIS and IR channel). It will therefore ensure an optimal performance of the coronagraph device.

- The Pupil Tip-Tilt loop corrects for pupil shift (telescope and instrument). It will ensure that the uncorrected instrumental aberrations effects (in the focal plane) will always be located at the same position and thus will be canceled out by a clever post-processing procedure.

- Non-Common Path Aberrations will be measured with phase diversity, and their pre-compensation will lead to the reduction of persistent speckle.

The 41x41 actuator High Order DM of 180 mm diameter has been manufactured and delivered by CILAS and displays a best flat of 5nm rms surface and maximum stroke > ±3.5 μm (Fig. 4). The high bandwidth (1 kHz) tip-tilt mirror (TTM) with ±0.5 mas resolution is being developed by the LESIA. The wavefront sensor is a 40x40 lenslet Shack-Hartmann, covering the 0.45-0.95 μm spectral range, and equipped with a focal plane spatial filter[3] continuously variable in size from λ/d to 3λ/d at 0.7 μm, where d is the sub-aperture diameter, for aliasing control. It is based on the dedicated 240x240 pixel electron multiplying CCD220 from EEV and will achieve temporal sampling frequency of 1.2 kHz with a

read-out-noise < 1 e⁻ and a 1.4 excess photon noise factor. At the heart of the AO system is a Real Time Computer (RTC) Called SPARTA: "Standard Platform for Adaptive optics Real Time Applications", the new generation RTC from ESO, providing a global AO loop delay <1 ms. SPARTA allows to control the 3 system loops but it will also provide turbulent parameters and system performance estimation as well all the relevant data for an optimized PSF reconstruction and a clever signal extraction from scientific data.
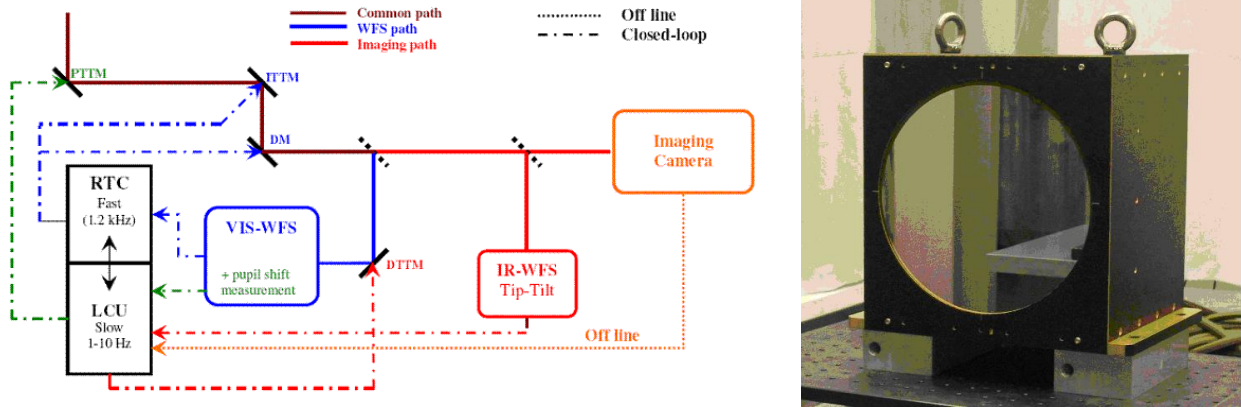

Fig. 4. The AO loop structure, with broad-band, NIR and VIS beams in brown, red, and blue resp. The fast (1.2 kHz) loop includes the DM, image tip-tilt (ITTM), Vis WFS and RTC. The RTC also generates a slow signal (1-10 Hz) for lateral pupil alignment via the pupil tip-tilt mirror (PTTM). Slow differential image motion between the Vis and NIR beams is detected by a NIR sensor, driving a differential tip-tilt plate (DTTP) that will offset the beam on the Vis WFS. The right picture shows the CILAS high order DM.

2.3. Coronagraphs

Coronagraphy is key for reaching our science goals. Its action is to reduce by a factor ≥100 the intensity of the stellar peak, and to eliminate the diffraction features due to the pupil edges. The baseline coronagraph suite will include an achromatic four-quadrant phase mask coronagraph (A4Q) based on precision mounting of four half-wave plates (HWP), and both a classical Lyot coronagraph (CLC) and an apodized Lyot coronagraph (ALC). Other options include the classical four-quadrant phase mask, which is now very well mastered and tested in the laboratory and on the sky with VLT/NACO. More explorative devices are also being investigated with options like a broad-band versions of the A4Q based on zero-order gratings or its circularly symmetric version, the annular groove phase mask (AGPM), both fabricated in micro-structured silicon and limited to the H and Ks bands. Because stellar coronagraphy is a quickly evolving field masks are exchangeable at all levels for future improvements.

The A4Q coronagraphs have now been prototyped[4] using the SPHERE f/40 focal and tested in monochromatic and polychromatic light in H, J and Y bands (Fig. 6). In the H band (R = 7) the nulling performance are very similar to that obtained in the monochromatic case at 1.55 µm, indicating the good achromatisation of the component. In the J and Y bands the nulling performance is decreased with a peak-to-peak attenuation of 350 and 315 respectively. However, contrast levels are quite homogeneous with respect to the H band, another indication of reasonable achromatization.

While the CLC option, with mask diameter of about 10λ/D, is within the realm of classical manufacturing, the ALC option requires an apodizer in the coronagraph entrance pupil. Prototyping is ongoing[5], and a promising technology using graded metal deposition has been identified. An alternative technology based on ion implantation is also considered, but this technology gives discrete steps in the apodization profile. The effects of this are being quantified by simulations.
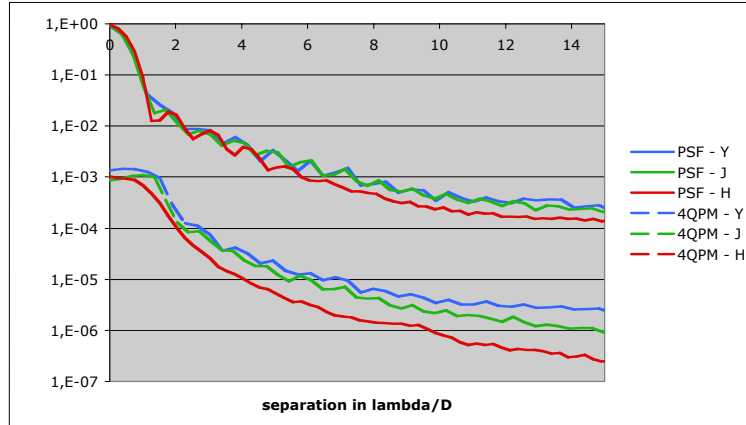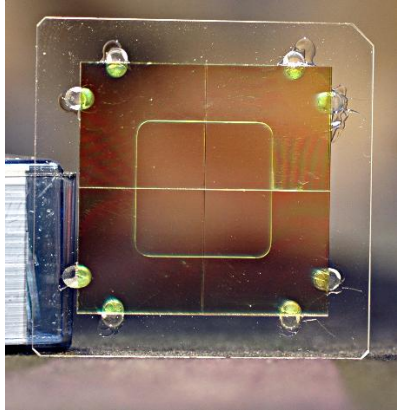
Fig. 5. SPHERE A4Q focal plane mask prototype. The left picture shows the complete assembled device (tungsten wires are placed to mask the edges of the wave plates). Right graph shows radial contrast in Y, J and H. The X-axis is scaled to each wavelength.

3. INFRARED DUAL IMAGING SPECTROGRAPH (IRDIS)

3.1. Overview

The IRDIS science module[6] covers a spectral range from 0.95-2.32 μm with an image scale of 12.25 mas consistent with Nyquist sampling at 950 nm. The FOV is 11" x 12.5", both for direct and dual imaging. Dual band imaging (DBI) is the main mode of IRDIS, providing images in two neighboring spectral channels with <10 nm rms differential aberrations. Two parallel images are projected onto the same 2kx2k detector with 18 μm square pixels, of which they occupy about half the available area. A series of filter couples is defined corresponding to different spectral features in modeled exoplanet spectra. The classical imaging (CI) mode allows high-resolution coronagraphic imaging of the circumstellar environment through broad, medium and narrow-band filters throughout the NIR bands including Ks. In addition to these modes, long-slit spectroscopy (LSS) at resolving powers of 50 and 500 is provided, as well as a dual polarimetric imaging (DPI) mode. A pupil-imaging mode for system diagnosis is also implemented.

All these modes require a coronagraph in the common path system and a corresponding Lyot stop in the IRDIS Lyot stop wheel. For the Long Slit Spectroscopy mode, the coronagraph mask is replaced by a coronagraphic slit. The slit is centered on the star, which is covered by a central patch, and a disperser device equipped with a dedicated Lyot stop is located in the IRDIS Lyot stop wheel. Two dispersion devices are provided, a double prism (same concept as in CONICA) for low resolution (LRS, ~50) and a grism for medium resolution (MRS, ~500). The prism can be used with either a YJHKs filter or a YJH filter, and the grism is used only with the YJH filter.

The main challenge of IRDIS is to achieve less than 10 nm differential aberrations between the two channels. An error budget based on high-quality polishing technology satisfies the requirement, and prototyping of DBI filters confirmed this budget. The beam-splitter option has been favored over the Wollaston option because it eliminates spectral blurring problems, which would limit the useful FOV, and allows the use of high-quality materials with high homogeneity.

The current opto-mechanical design of the IRDIS optical bench is shown in Fig. 8 (a). The entrance pupil coincides with the coronagraphic exit pupil (Lyot stop). Located in a collimated beam of diameter 10 mm, it constitutes the main optical interface with the common path optics. Beam splitter and imaging optics is located in a compact unit, allowing minimal thermal gradients and optimal mechanical stability. The detector is mounted on a two-axis translation stage to allow dithering for flat-field improvement. PI piezo motors, currently undergoing cryogenic qualification, power this stage, whose development is based on CONICA heritage. The cryostat concept is shown in Fig. 8 (b). A liquid nitrogen tank provides cooling power with capacity for 30h autonomy. The detector will be kept at ~80K, and the optics is stabilized at a temperature of around 100K to limit thermal background. The interface with the common path bench is ensured via a bracket fixed on the side of the table. IRDIS is fixed to this bracket via a hexapod structure that is very stiff and allows six degrees of freedom for position adjustment.
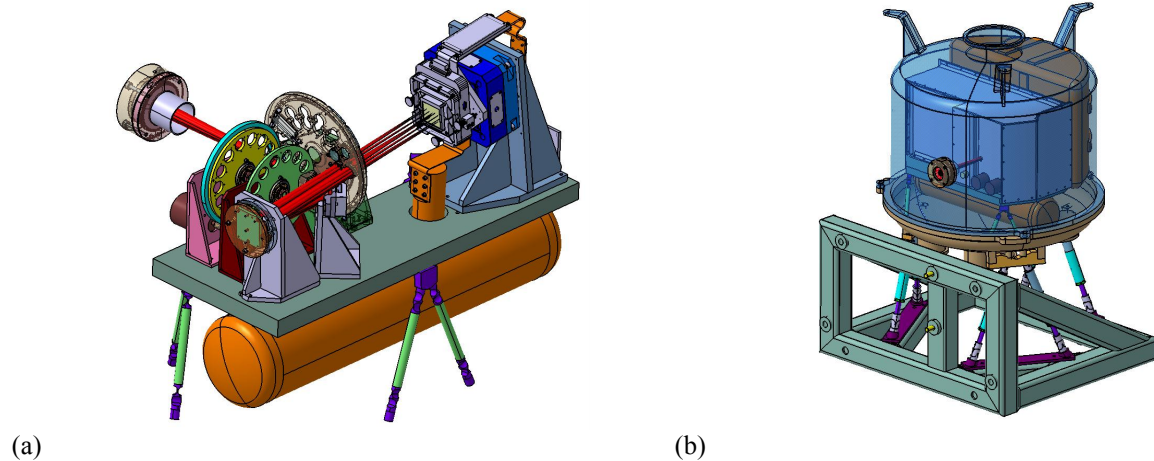
(a)   (b)

Fig. 6. View of the IRDIS optical bench (a) and cryostat (b).

3.2. Dual-band imaging performance

Numerical simulations of the IRDIS performance have been made using the SPHERE CAOS module[7,8]. Typical simulated DBI images are shown in Fig. 7. For this mode, the Top Level Requirement is a 5σ contrast of $5 \cdot 10^{-5}$ at 0.1" and $5 \cdot 10^{-6}$ at 0.5" from the star in 1-hour integrations achieved by imagery at both sides of the H-band methane absorption edge. High contrast imaging has to deal at first order, with two components: a speckled halo which is averaging over time and a static speckle pattern originating from quasi-static aberrations evolving occurring with a much longer lifetime than atmospheric residuals. Because the DBI mode is performing simultaneous differential imaging, performances are mostly limited by the quasi-static aberrations upstream the coronagraph and by the spectral separation between DBI filters.

Fig. 8 shows plots of different companions intensity compared with radial variance profiles in the processed images. We consider an integration time of 1-hour and the achievable contrast and signal to noise ratio of several models of planets in various conditions. At 1.6 µm and for bright sources, not limited by photon noise, it is expected to reach a 5σ contrast of $\sim 2 \cdot 10^{-5}$ at its inner working angle of 0.1", and $\sim 5 \cdot 10^{-7}$ at 0.6".
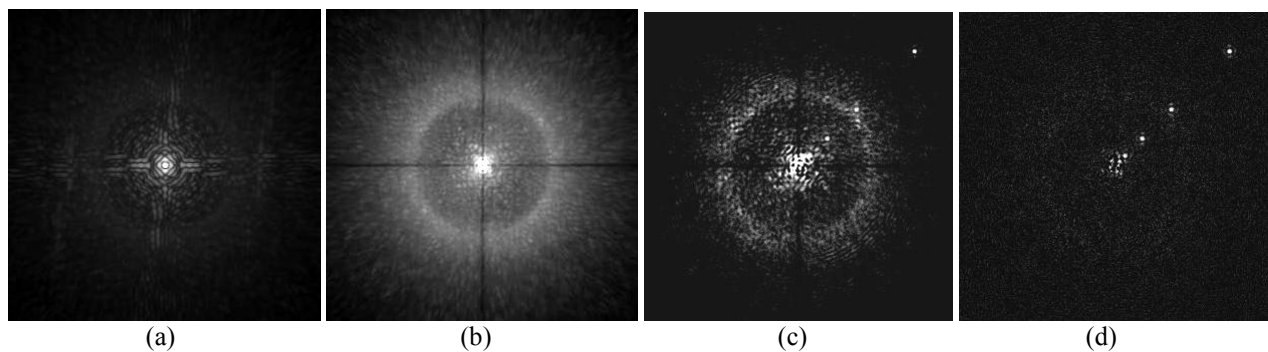

(a)   (b)   (c)   (d)

Fig. 7: M0V star 10pc image with DBI (H2H3). The detected planets are located at 0.1", 0.2", 0.5", 1", 2" from the star and correspond to 1MJ at 10My - 3MJ at 100My - 11MJ at 1Gy - 25MJ at 5Gy. The illustrations show the star PSF (a), the 4QPM raw image (b), the 4QPM single subtraction of 2 wavelengths H2H3 (c), the double subtraction image including calibration of differential aberrations and chromatic residual (d). Gray scales are arbitrary.
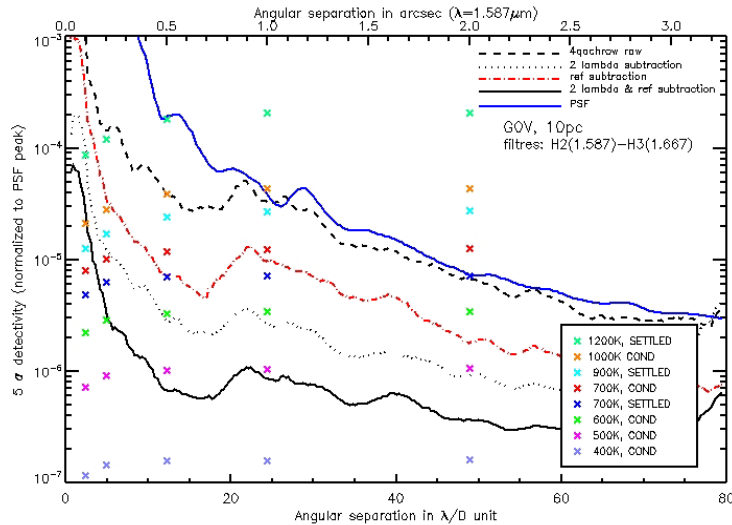
Fig. 8: Estimated detectivity at 5σ in 1h for various models of planets, for a G0V star at 10pc observed in dual band imaging (H2H3). COND refers to models for a condensed atmosphere free of dust, SETTLED refers to atmospheres with rainout of refractory material.

4. INTEGRAL FIELD SPECTROGRAPH (IFS)

IFS are very versatile instruments, well adapted for spectroscopic differential imaging as needed for detection of planets around nearby stars. The main advantage of IFS is that differential aberrations can be kept at a very low level; this is true in particular for lenslet based systems, where the optical paths of light of different wavelength within the IFS itself can be extremely close to each other. Additionally, IFS provide wide flexibility in the selection of the wavelength channels for differential imaging, and the possibility to perform spectral subtraction, which in principle allows recovering full information on the planet spectra, and not simply the residual of channel subtraction, as in classical differential imagers. The main drawback of IFS is that they require a large number of detector pixels, resulting in a limitation in the field of view, which is more severe for lenslet-based systems. Classical differential imagers and IFS are then clearly complementary in their properties, and an instrument where both these science modules are available may be extremely powerful for planet search.

Both a classical TIGER[9] and an innovative BIGRE[10] concept have been considered for the SPHERE IFS[11], the latter being finally selected because of its better properties. Both these designs are based on lenslet systems: in the case of TIGER design the array of micropupil images created by the lenslet array are imaged on the detector, after having being dispersed; in the case of the BIGRE array, a second lenslet array allows formation of pseudo-slit images corresponding to a very small portion of the field, which are then imaged on the detector after being dispersed. The main advantage of the BIGRE concept is that the pseudo-slit images are only very mildly dependent on wavelength and have a quasi-top-hat profile, while in the TIGRE concept the micropupil images are diffraction images with secondary maxima, whose size is dependent not only on wavelength, but also on the illumination of the individual lenslets. The BIGRE system allows a better control of diffraction effects and a much lower level of cross-talk. Achievement of specifications of the BIGRE concept was proven with a laboratory prototype at INAF-OAPD.

The 5-σ detectivity of the IFS at 0.5" is from 10^{-6} to 10^{-7} with respect to the un-occulted PSF peak, depending on star and observing conditions[12]. A resolving power per pixel of ~100 is obtained, with a 1.77" (side) square FOV. Nyquist-limited spatial sampling at 0.95 μm is imposed as for IRDIS. Optimized commonality between IFS and IRDIS in terms of detector and associated equipment is seen as an important system goal. The same 2kx2k detector format is therefore adopted, and the long-wavelength cut off defined for IRDIS is also acceptable for IFS.

In addition to the micro-lens system at the entrance of the spectrograph, the opto-mechanical concept includes collimation optics, an Amici Prism providing zero beam deviation and constant resolution within the entire wavelength range, camera optics, and the detector cryostat (Fig. 9). Thermal background is controlled by extending the cryostat >150mm in front of the detector, thus limiting the solid angular view of the warm environment, and by including a cold

short-pass filter. Detector dithering (in order to improve flat-field precision) is achieved by small movements of the camera optics, realized by commercial piezo's.
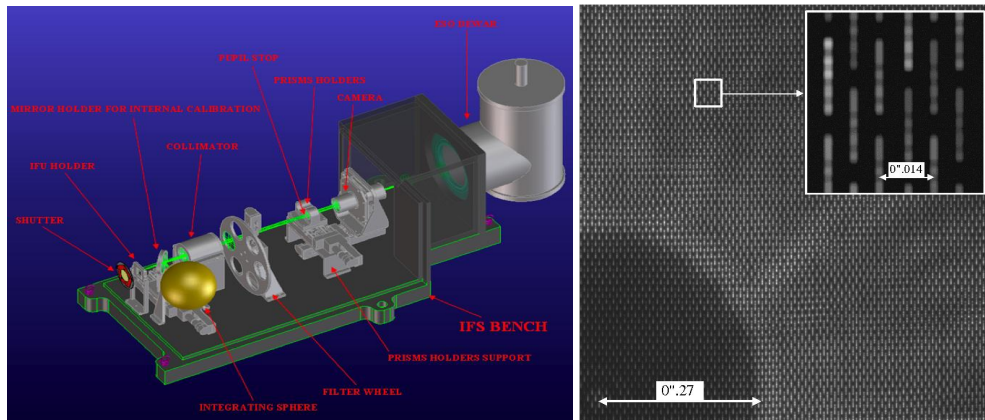

Fig. 9. Opto-mechanical design of the IFS (left) and a portion of a simulated detector image (right).

5. ZURICH IMAGING POLARIMETER (ZIMPOL)

5.1. Overview

ZIMPOL[13] is located behind SPHERE visible coronagraph. Among its main specifications are a bandwidth of 600-900 nm and an instantaneous field of view of 3 x 3 arcsec^2 with access to a total field of view of 8" diameter by an internal field selector. The ZIMPOL optical train contains a common optical path that is split with the aid of a polarizing beamsplitter in two optical arms. Each arm has its own detector. The common path contains common components for both arms like calibration components, filters, a rotatable half wave plate and a ferroelectric liquid crystal polarization modulator. The two arms have the ability to measure simultaneously the two complementary polarization states in the same or in distinct filters. The images on both ZIMPOL detectors are Nyquist sampled at 600 nm. The detectors are both located in the same cryostat and cooled to -80°C. The rest of the ZIMPOL opto-mechanical system is at ambient temperature.

The basic ZIMPOL principle for high-precision polarization measurements includes a fast polarization modulator with a modulation frequency in the kHz range, combined with an imaging photometer that demodulates the intensity signal in synchronism with the polarization modulation. The polarization modulator and the associated polarizer convert the degree-of-polarization signal into a fractional modulation of the intensity signal, which is measured in a demodulating detector system by a differential intensity measurement between the two modulator states. Each active pixel measures both the high and the low states of the intensity modulation and dividing the differential signal by the average signal eliminates essentially all gain changes, notably changes of atmospheric transparency or electronic gain drifts.

For the SPHERE implementation (Fig. 10), the modulator is a ferroelectric liquid crystal working at a frequency of about 1 kHz. The demodulator is a special CCD camera, which measures for each active pixel the intensity difference between the two modulation states. For achieving this, every second row of the CCD is masked so that charge packages created in the unmasked row during one half of the modulation cycle are shifted for the second half of the cycle to the next masked row, which is used as temporary buffer storage (the CCD can be equipped with cylindrical micro-lenses which focus the light onto the open CCD rows). After many thousands of modulation periods the CCD is read out in less than one second. The sum of the two images is proportional to the intensity while the normalized difference is the polarization degree of one Stokes component. Because the measurement is fully differential, systematic error sources are reduced to a very low level (on the order 10^{-5}). The main requirement is that the incoming signal is not strongly polarized ($p<10^{-2}$).

5.2. ZIMPOL performance

Simulations of the ZIMPOL performances have been conducted for various test cases[13]. The detectivity curves for one of these cases (G0V star at 3 pc, classical Lyot coronagraph, 4h observation time) are presented in Fig. 11. In the double-

difference image (curve C), a spurious background landscape caused by the combination of static, polarized and temporal aberrations still obscures any planet signals. Angular differential imaging is necessary to reduce this background to a level where planets can be detected. In the worst-case scenario of a double-difference background fluctuating on the time scale of field rotation, only angular averaging is possible. Curves D and E show the performance for active field rotation over 23 discrete positions and for natural field rotation over a continuous arc of 45∘, respectively. In either case, the best-case scenario is a complete elimination of the aberration-dominated background, leaving only the photon noise (curve F). The detection zone for planets ranges from 0.08" (the edge of the 5 λ/D coronagraph) to 0.3" (the control radius of the AO). The S/N ratios improve with decreasing angular separation. At the photon limit, a 25% polarized Jupiter-sized planet is detectable at 0.3" with ~5σ confidence; at 0.1", the same planet reaches ~50σ.
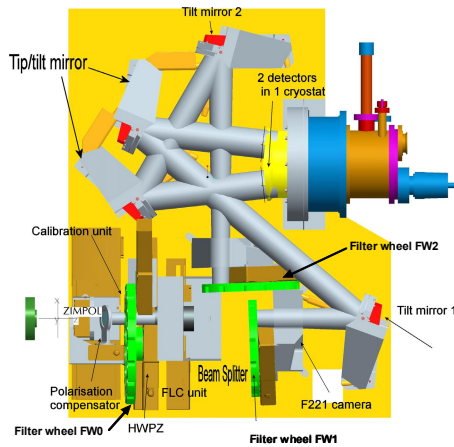

Fig. 10. ZIMPOL opto-mechanical design.

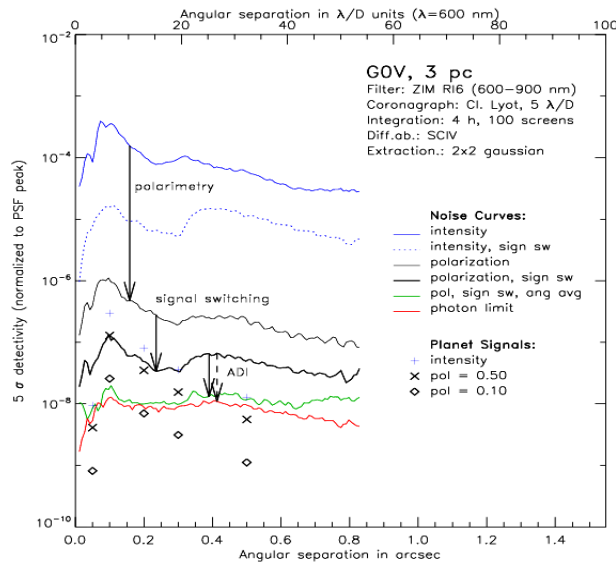

Fig. 11. Performance plot for a G0V star at 3 pc with a Lyot coronagraph with 5 λ/D mask radius at λ=600 nm, 4h of observation. The curves show the level at which a signal is detected with a confidence of 5σ. The simulated broadband images were composed from 30 monochromatic PSFs, convolved with a Gaussian aperture of 2 pix width to suppress noise below the spatial scale of planet signals.

6. OBSERVING MODES AND STRATEGY

Three main observing modes have been defined in order to draw the maximum benefit of the unique instrumental capabilities of SPHERE.

The *NIR survey mode* is the main observing mode which will be used for ~80% of the observing time. It combines IRDIS dual imaging in H band with imaging spectroscopy using the IFS in the Y-J bands. This configuration permits to benefit simultaneously from the optimal capacities of both dual imaging over a large field (out to ~5" radius) and spectral imaging in the inner region (out to at least 0.7" radius). In particular, it allows to reduce the number of false alarms and to confirm potential detections obtained in one channel by data from the other channel. This will be a definitive advantage in case of detections very close to the limits of the system.

The *NIR characterization mode*, in which IRDIS is used alone in its various modes, will allow obtaining observations with a wider FOV in all bands from Y to short-K, either in dual imaging or dual polarimetry, or in classical imaging using a variety of broad and narrow-band filters. This will be especially interesting in order to obtain complementary information on already detected and relatively bright targets (follow-up and/or characterization). Spectroscopic characterization at low or medium resolution will be possible in long-slit mode. Additional science cases will also benefit from these observing modes (disks, brown dwarfs, etc.).

The visible search and characterization mode, will benefit from ZIMPOL polarimetric capacities to provide unique performance in reflected light very close to the star, down to the level required for the first direct detection in the visible of old close-in planets, even if on a relatively small number of targets. ZIMPOL also provides classical imaging in the visible, offering unique high-Strehl performance.

7. CALIBRATION, DATA REDUCTION AND HANDLING

SPHERE is a highly specialized instrument that stretches the control of technical tolerances to the limits both during the design and manufacturing phases, and particularly during its many extensive calibration procedures. It is clear, that with such an instrument the greatest care must be taken to ensure that the quality of the data taken at the telescope indeed matches the excellence of the instrument itself.

This is why it was decided that SPHERE needed a rather unique ``Data Reduction and Handling" (DRH) software package[14] which accompanies the data from the preparation of the observing program, i.e. optimizing target lists, preparing and scheduling observations and calibrations, to the reduction of raw data as they come from the instrument detectors, to the analysis and search for planetary signals and the final inclusion of detected candidates in the target lists and the scheduling of follow-up observations. This end-to-end approach is particularly critical for the surveys envisioned to fulfil the SPHERE science goals in terms of statistical properties of the detected planets.

Specifically during the reduction of both calibration and science data, strict error propagation control is designed into the DRH software in order to enable sophisticated analysis and planet signal search by modelling all instrumental and atmospheric properties. This will ensure an homogenous quality of (non-)detections achieved with SPHERE and will enable re-processing of all data when improved versions of the analysis procedures become available.

8. SPHERE PROJECT ORGANISATION AND SCHEDULE

SPHERE is built by a consortium of 11 institutes of 5 European countries, together with ESO which is both the final customer and a formal partner in the project. The consortium is made of the following entities: LAOG (P.I. institute, Grenoble, France), MPIA (Co-P.I. institute, Heidelberg, Germany), LAM (Marseille, France), LESIA (Paris, France), Fizeau (Nice, France), Osservatorio Astronomico di Padova/INAF (Padova, Italy), Observatoire de Genève (Geneva, Switzerland), ETHZ (Zurich, Switzerland), University of Amsterdam (Amsterdam, The Netherlands), NOVA/ASTRON (Dwingeloo, The Netherlands) and ONERA (Chatillon, France).

The kick-off meeting took place in March 2006, the Preliminary Design Review in September 2007 and the Optical Final Design Review in May 2008. The Final Design Review for the whole project is expected to take place at the end of 2008 and the current development plan foresees a delivery to ESO by the end of 2010 and the first light for SPHERE in the spring of 2011.

9. CONCLUSION

We have presented here the status of the SPHERE instrument, shortly before it undergoes its Final Design Review by the end of 2008. Development and prototyping of keystone elements has been successful and all top-level requirements are now expected to be met. The manufacturing and integration process will start in early 2009 for a delivery to ESO by the end of 2010 and beginning of operation in the spring of 2011.

REFERENCES

1. Emmanuel Hugot, Marc Ferrari, Kacem El-Hadi, Gérard R. Lemaître, Pierre Montiel, "Stress polishing of toric mirrors for the VLT-SPHERE common path", in *Advanced Optical and Mechanical Technologies in Telescopes and Instrumentation*, SPIE 7018-5 (2008)
2. Cyril Petit, Thierry Fusco, Jean-Marc Conan, Jean-François Sauvage, Gérard Rousset, Pierre Gigan, Julien Charton, David Mouillet, Patrick Rabou, Markus E. Kasper, Enrico Fedrigo, Norbert Hubin, Philippe Feautrier, Jean-Luc Beuzit, Pascal Puget, "The SPHERE XAO system: design and performance", in *Adaptive Optics Systems*, SPIE 7015-65 (2008)
3. Thierry Fusco, Cyril Petit, Patrick Rabou, Kjetil Dohlen, David Mouillet, Pascal Puget, "Optimization of a spatially filtered Shack-Hartmann wavefront sensor", in *Adaptive optics systems*, SPIE 7015-54 (2008)
4. Anthony Boccaletti "Prototyping achromatic coronagraphs for exoplanet characterization with SPHERE", in *Adaptive Optics Systems*, SPIE 7015-46 (2008)
5. Géraldine Guerri, Sylvie Robbe-Dubois, Jean-Baptiste Daban, Lyu Abe, Richard Douet, Philippe Bendjoya, Farrokh Vakili, Marcel Carbillet, "Apodized Lyot coronagraph for the VLT instrument SPHERE: laboratory tests and performances of a first prototype in the visible", in *Ground-based and Airborne Instrumentation for Astronomy II*, SPIE 7014-124 (2008)
6. Kjetil Dohlen, Maud P. Langlois, Michel Saisse, "The infra red dual imaging and spectrograph for SPHERE: design and performance", in *Ground-based and Airborne Instrumentation for Astronomy II*, SPIE 7014-126 (2008)
7. Carbillet, M.; Verinaud, Ch.; Guarracino, M.; Fini, L.; Lardiere, O.; Le Roux, B.; Puglisi, A. T.; Femenia, B.; Riccardi, A.; Anconelli, B.; Correia, S.; Bertero, M.; Boccacci, P., "CAOS: a numerical simulation tool for astronomical adaptive optics (and beyond)" in *Advancements in Adaptive Optics*. Proc. SPIE 5490, pp. 637 (2004).
8. Marcel Carbillet, Anthony Boccaletti, Christian Thalmann, Thierry Fusco, Arthur Vigan, David Mouillet, " The software package SPHERE: a numerical tool for end-to-end simulations of the VLT instrument SPHERE", in *Adaptive Optics Systems*, SPIE 7015-256 (2008)
9. Bacon, R, "The integral field spectrograph TIGER: results and prospects. In: *3D Optical Spectroscopy Methods in Astronomy*, G. Comte, M. Marcelin (eds), ASP Conf. Series 71, 1995, p. 239
10. Enrico Giro, Riccardo U. Claudi, Jacopo Antichi, Pietro Bruno, Enrico Cascone, Vincenzo De Caprio, Silvano Desidera, Raffaele G. Gratton, Dino Mesa, Salvatore Scuderi, Massimo Turatto, Jean-Luc Beuzit, Pascal Puget, "BIGRE: a new double microlens array for the integral field spectrograph of SPHERE", in *Ground-based and Airborne Instrumentation for Astronomy II*, SPIE 7014-125 (2008)
11. Riccardo U. Claudi, Massimo Turatto, Raffaele G. Gratton, Jacopo Antichi,; Enrico Cascone,; Vincenzo De Caprio,; Silvano Desidera, Dino Mesa, Salvatore Scuderi, "SPHERE IFS: the spectro differential imager of the VLT for exoplanets search", in *Ground-based and Airborne Instrumentation for Astronomy II*, SPIE 7014-119 (2008)
12. S. Desidera, R. Gratton, R. Claudi, J. Antichi, D. Mesa, M. Turatto,; P. Bruno, E. Cascone,; V. De Caprio,; E. Giro; S. Scuderi; M. Feldt, A. Pavlov, K. Dohlen, J-L Beuzit, D. Mouillet, P. Puget, F. Wildi, "Calibration and data reduction for planet detection with SPHERE-IFS", in Ground-based and Airborne Instrumentation for Astronomy II, SPIE 7014-127 (2008)
13. Christian Thalmann, Hans M. Schmid, Anthony Boccaletti, David Mouillet, Kjetil Dohlen, Ronald Roelfsema, Marcel Carbillet, Daniel Gisler, Jean-Luc Beuzit, Markus Feldt, Raffaele Gratton, Franco Joos, Christoph U. Keller, Jan Kragt, Johan H. Pragt, Pascal Puget, Florence Rigal, Frans Snik, Rens Waters, Francois Wildi, "SPHERE ZIMPOL: Overview and performance simulation", in *Ground-based and Airborne Instrumentation for Astronomy II*, SPIE 7014-120 (2008)
14. Aleksei I. Pavlov, Markus Feldt, Jean-Luc Beuzit, David Mouillet, Franco Joos, Silvano Desidera, Thomas F. E.Henning, "SPHERE data reduction and handling system: overview, project status and development", in *Advanced Software and Control for Astronomy*, SPIE 7019-130 (2008)